JOURNAL OF GEOPHYSICAL RESEARCH, VOL. 96, NO. B10, PAGES 16,625–16,639, SEPTEMBER 10, 1991

The Relationship Between Plate Curvature and Elastic Plate Thickness: A Study of the Peru-Chile Trench

ANNE V. JUDGE[1] AND MARCIA K. MCNUTT

Department of Earth, Atmospheric, and Planetary Sciences, Massachusetts Institute of Technology, Cambridge, Massachusetts

The age of the Nazca plate where it enters the Peru and northern Chile trenches varies from 30 Ma in the north to 45 Ma in the south as its dip beneath the South American continent steepens from 13° to 30°. If the elastic thickness T_e of oceanic lithosphere depends only on its age, and therefore thermal state, we would expect that T_e determined from fitting the flexure of the lithosphere over the outer rise as revealed in the depth, geoid, and gravity anomalies would increase from the Peru Trench in the north to the northern Chile Trench further south. We find that the opposite is true: the lithosphere appears stiffer outboard of the Peru Trench than it does offshore Chile. To explain deflections of the lithosphere seaward of Peru, the isotherm controlling the elastic/ductile transition must be near 800°C, providing the thermal structure of the plate is that predicted by the standard thermal plate model. Because the decrease in plate stiffness to the south is correlated with an increase of plate curvature over the outer rise and outer trench wall, we interpret our result in terms of inelastic yielding of the oceanic lithosphere when bent to high strains. The magnitude of the reduction in strength, however, suggests that the standard oceanic yield strength envelope underestimates the amount of failure for lithosphere bent to high strains unless the stress field off northern Chile is characterized by 100-MPa-level tension. The more highly bent segment of subducting lithosphere at this trench also dips at a steeper angle at greater depth beneath the continent, but detailed analysis of plate geometry does not support a relationship between slab dip as determined by earthquake hypocenters and elastic behavior over the outer rise.

INTRODUCTION

It is generally agreed that oceanic lithosphere behaves as a thin elastic plate in response to applied stress over geologic time scales [*Walcott*, 1970; *Hanks*, 1971; *Watts and Cochran*, 1974; *Caldwell et al.*, 1976] and that the effective elastic thickness of the plate increases as the square root of age of the plate at the time of loading due to thermal control on the depth to the elastic-ductile transition [*Watts et al.*, 1980]. What is less certain is the magnitude of the reduction in the effective elastic thickness from the value predicted by lithospheric age due to inelastic processes within sharply bent plates at subduction zones, despite a number of attempts to explicitly include plastic deformation in flexural models [*Turcotte et al.*, 1978; *McAdoo et al.*, 1978; *Bodine and Watts*, 1979; *Carey and Dubois*, 1981] and the rheological arguments for its importance [*Goetze and Evans*, 1979; *McNutt and Menard*, 1982]. A better calibration of the yield strength of oceanic lithosphere is essential for understanding its rheology and state of stress.

The Peru-Chile Trench (Figure 1) provides a suitable natural laboratory for investigating lithospheric rheology, for as the age of the subducted Nazca plate increases from 30 Ma to 45 Ma to the south along the trench system [*Handschumacher*, 1976; *Hilde and Warsi*, 1984; *Herron*, 1972; *Scheidegger and Corliss*, 1981], the curvature of the plate on the outer rise and outer trench wall increases to accommodate a change from 13° to 30° in the dip of the downgoing slab beneath South America [*Barazangi and Isacks*, 1976, 1979]. Using observations of depth, geoid, and gravity anomalies, we will examine what constraints can be placed on the relative importance of temperature and bending stress in controlling effective elastic plate thickness. If failure of the plate at the higher stresses sustained in the south is unimportant, then the effective elastic plate thickness of that older lithosphere should be at least 5 km greater than that of the younger lithosphere to the north. If failure of the plate at high curvatures is more important than the 15 m.y. increase in age in controlling elastic plate thickness, then the effective elastic plate thickness to the south may actually be less than that of the younger lithosphere in the north.

THE MODEL

We begin by approximating the lithosphere as a one-dimensional thin elastic plate overlying a fluid mantle flexed by external forces and moments applied at the trench axis [*Caldwell et al.*, 1976; *Turcotte and Schubert*, 1982]. The elastic strength of such a plate is measured by its flexural rigidity D, which is related to the effective elastic plate thickness T_e via $D = E T_e^3/12(1-\nu^2)$, where E is Young's modulus and ν is Poisson's ratio. Its displacement w at a point x external to the loads is described by a solution to the thin plate equation

$$w(x) = A \exp\left(-\frac{x}{\alpha}\right) \sin\frac{x}{\alpha} \qquad (1)$$

where $\alpha^4 = (4D/\Delta\rho g)$, $\Delta\rho$ is the difference in density between the underlying mantle rock and the overlying water, g is the gravitational acceleration, A depends on the magnitude of all forces and moments applied landward of the trench axis, and x is measured from the first zero crossing seaward of the trench axis [*Turcotte et al.*, 1978; *Jones et al.*, 1978; *Turcotte and Schubert*, 1982]. This solution is only valid if the flexural rigidity is constant and there are no lateral forces applied to the plate.

The predicted bathymetry from elastic flexure is given directly by (1). The corresponding geoid and gravity anomalies can be generated using *Parker*'s [1972] method to calculate potential field anomalies from undulations of the surface and Moho as described by (1) seaward of the trench axis and by reflecting the profile about this point landward of the trench axis [*McAdoo and Martin*, 1984].

[1]Now at Geophysical Research, ELF Aquitaine, Pau, France.

Paper number 90JB01772.
0148-0227/90/90JB-01772$05.00

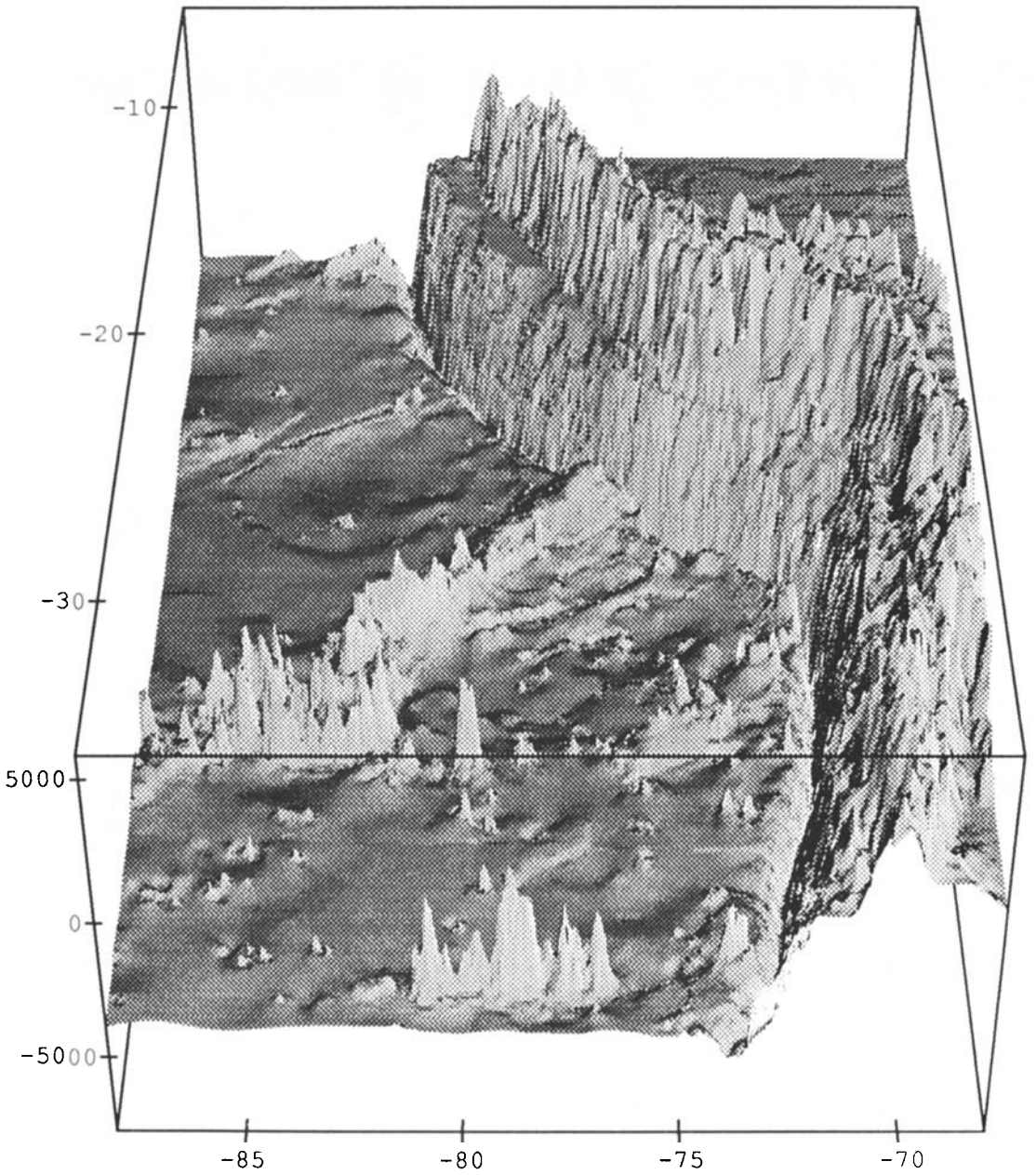

Fig. 1. Three-dimensional image of the topographic relief along the western coast of South America. The region referred to as the Peru province lies to the north of the northeast-trending Nazca Ridge, and the region referred to as the Northern Chile province lies to the south.

This approach gives similar results to a model in which the Moho deepens landward of the trench, and has the advantage of being easily reproducible, whereas an arbitrary choice of slope under the inner trench wall is not.

By varying both α and A, we can estimate the value of T_e which best explains the bathymetric, geoid, or gravity undulations seaward of the subduction zone. In most cases the portion of the bathymetric, geoid, or gravity profile to which the theoretical curve (1) was fit extended from the trench axis to a point 300 km seaward of the origin (second zero-crossing). In some cases a slightly shorter segment was used in order to avoid features, such as seamounts, which were obviously unrelated to the flexural response of the plate. These profiles included nearly undeflected seafloor as well as sharply bent lithosphere near the base of the trench. For each profile, a curve of minimum rms misfit versus elastic thickness was constructed by varying amplitude A until misfit was minimized for the value of α corresponding to each elastic thickness. The uncertainty assigned to each T_e-estimate is one-half the width of this curve where the misfit reached 1.5 times its minimum value, as shown in Figure 2. This measure was chosen because it is dependent on both the steepness of this curve and the minimum value the misfit obtains. A profile which is fit with small minimum misfit and a relatively wide, shallow curve (Figure 2*a*) and a profile fit with large misfit but a steep curve (Figure 2*b*) can both be considered to have a well-constrained elastic thickness and will both have a narrow half-width as determined by this method. In general, profiles for which the half-width was less than 10 km were considered to have a well-constrained value for T_e.

For profiles along which the flexural stresses are insufficient to exceed the strength of the lithosphere at depths shallower than the base of the elastic plate, T_e should correspond to the depth to some isotherm Θ_e that corresponds to the elastic/ductile transition and deepens as the square root of the age of the plate [*Watts et al.*, 1980]. Any yielding of the plate, such as via brittle failure near the

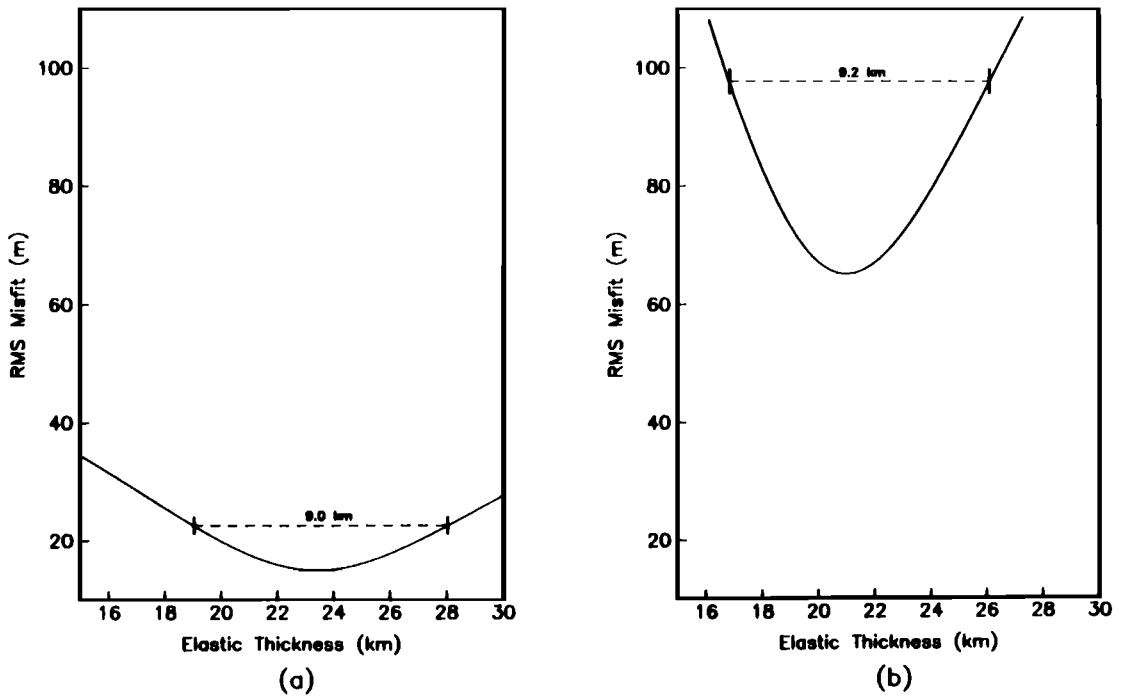

Fig. 2. (*a*) A plot of the minimum misfit at each value of elastic thickness for profile 3 in the northern region of the Peru province. The half-width is 4.5 km. (*b*) A similar plot for profile 5 in region 2 of the North Chile province. The half-width is 4.6 km.

upper surface or ductile creep near the base, in response to large elastic fiber stresses will cause T_e to underestimate the depth to the isotherm Θ_e. Thus given observations of changes in T_e with lithospheric age and curvature (the second derivative of the deflection w) along the Peru-Chile Trench, we can estimate the value of Θ_e and assess the magnitude of the reduction in the effective elastic plate thickness T_e caused by yielding of the lithosphere at high stresses [*Goetze and Evans*, 1979; *McNutt and Menard*, 1982].

THE DATA

In order to study flexure of the plate seaward of the Peru-Chile Trench, we extracted profiles perpendicular to the trench axis from global data sets of bathymetry [*Heirtzler and Edwards*, 1985], geoid [*Marsh et al.*, 1986], and gravity derived from geoid using the method of *Haxby* [1987]. We found that modeling three different types of data was useful for distinguishing which features of the profiles were unrelated to plate flexure. For example, seamounts and plateaus often led to a poor fit between the predictions of (1) and a bathymetric profile, but since those features are isostatically compensated, they were less apparent in the geoid profile. In addition, even though the geoid and gravity are only different representations of the same altimetric data set, the geoid proved to be sensitive, even at points far from the trench, to the exact configuration of mass assumed landward of the trench axis, whereas the gravity over the outer rise and even over most of the trench wall was insensitive to this geometry.

The gridded bathymetric data were originally interpolated from shipboard readings along tracks that provide generally good coverage of the area. The separation of ship tracks parallel to the trench is usually less than 30 km, whereas characteristic shapes of trench-related structures in that dimension in most cases can be traced over 80 km. We interpolated the bathymetric data onto profiles spaced at 10-km intervals perpendicular to a number of line segments fit to the trench axis. An attempt was made to subtract an age-depth curve from these profiles, but they had no apparent slope with age despite the young age of the crust.

Geoid and gravity data were obtained on a 15-min grid and interpolated onto profiles spaced 30 km apart, corresponding to every third bathymetric profile across the trench axis. A model GEM-T1 [*Marsh et al.*, 1988] reference field to degree and order 10 was removed from the geoid data. Removal of higher-order fields produced a geoid with no apparent relationship to the outer rise. After removal to degree and order 10, a long-wavelength variation was still apparent across the region of interest. Because this trend did not appear to relate to the topography of the outer rise and trench, and its slope was greater than that of the geoid-age relationship in young crust, it was simply removed by subtracting from each profile a line of constant slope.

RESULTS

We first present the results from modeling the depth, geoid, and gravity data from the Nazca plate seaward of the Peru and northern Chile trenches assuming two-dimensional flexure of a plate with constant rigidity and no applied in-plane stress. Enough profiles are adequately fit under these restrictive assumptions to estimate the elastic plate thickness and plate curvature in each area. However, at the end of this section we do discuss the effect of relaxing these assumptions to allow variable plate rigidity, three-dimensional bending, and horizontal thrusts.

Peru

The Peru trench can be approximated as a 300-km-long northern segment running from 6°S and 8.5°S and a 600-km-long southern segment continuing to 13.2°S, where the trench becomes shallower and less well-defined approaching the flanks of the Nazca Ridge (Figure 3). Some representative bathymetric profiles crossing the trench are shown in Figure 4, and the geoid profiles along the same tracks appear in Figure 5. The bathymetric profiles are numbered consecutively from north to south within each region.

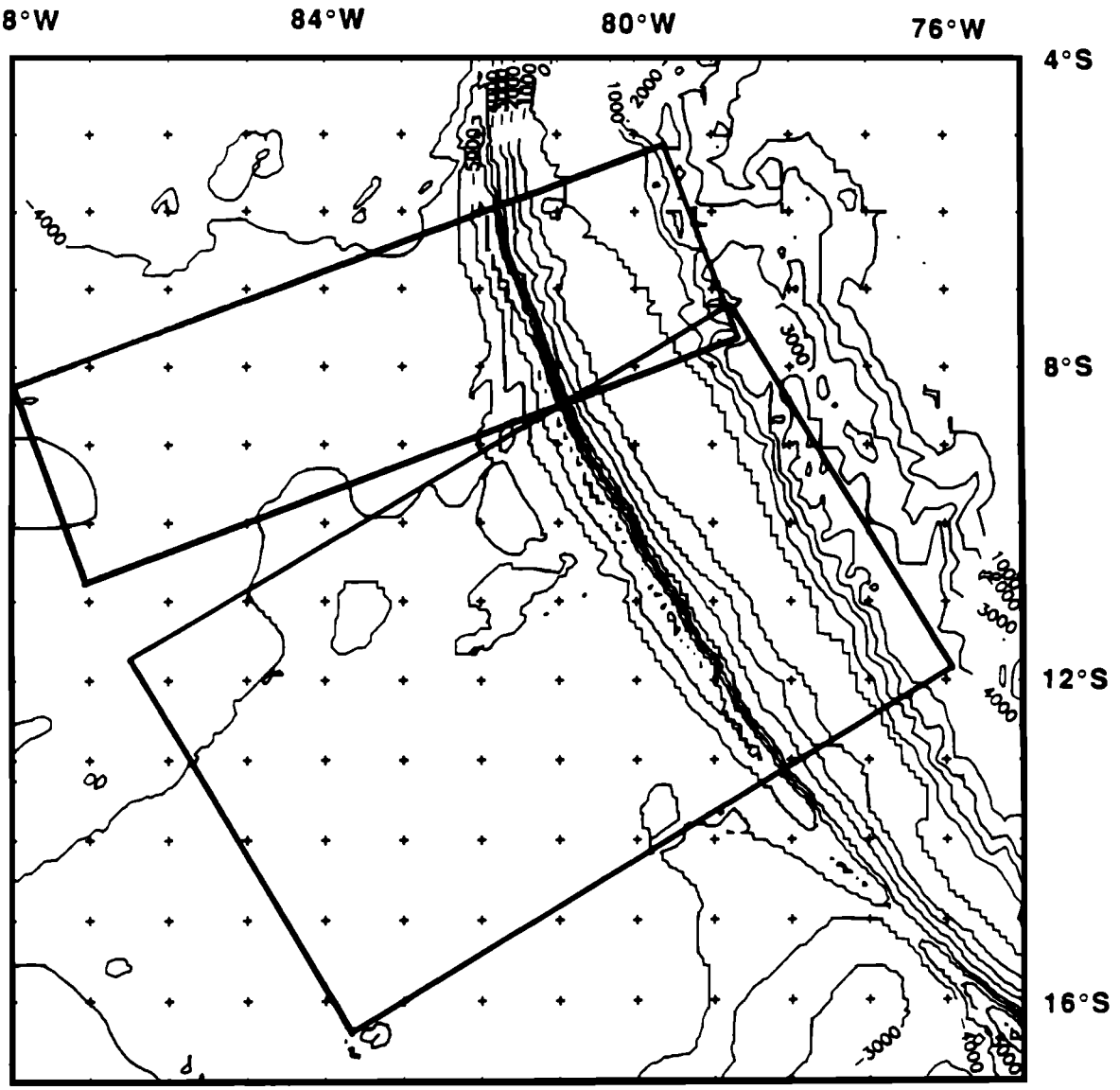

Fig. 3. Bathymetry of the region near the Peru Trench for which data were obtained, showing the location of the areas from which profiles were taken

Geoid height profiles are identified by the number of the corresponding bathymetric profile. Those profiles which could be fit by elastic theory are shown with the best fitting elastic curve superimposed, and the values for T_e are plotted in Figures 6*a* and 6*b*.

In general, there is fairly good agreement among the elastic plate thickness estimates derived from bathymetry, geoid, and gravity data for northern Peru, although there is a tendency for geoid data to indicate larger values of T_e and for bathymetry to indicate smaller values compared to those consistent with the gravity data (Figure 6*a*). Also, there is a monotonic decrease in elastic plate thickness determined from bathymetric data over the northernmost 100 km of the northern Peru Trench that is not indicated by the geoid or gravity data, which in general are more consistent across the area.

Only bathymetric profiles in the northernmost 250 km of the southern region (Figure 6*b*) could be fit by the elastic model, while nearly all of the geoid and gravity profiles displayed clear outer rises consistent with the shape predicted by (1). Even where the bathymetric profiles could be fit with an elastic model, the values for T_e are much smaller than those indicated by either geoid or gravity. Throughout the southern region, the outer rise in the bathymetry is small or nonexistent, and its disappearance cannot be explained by sediment thickness patterns [*Hussong et al.*, 1976; *Dang*, 1984]. The inconsistency between the small value for elastic thickness obtained from the bathymetry and the presence of distinct geoid and gravity highs indicates that the bathymetry does not reflect the behavior of the plate, and for this reason values derived from bathymetry were excluded in computing the average elastic thickness in the Peru province.

Near the northern edge of the southern region the Mendaño Fracture Zone intersects the trench, with an associated change in crustal age of 12 Ma. Averaging values of elastic thickness found for same-age crust results in a value of 32 ± 4 km for the 30-Ma lithosphere of the northern region and 39 ± 2 km for the 42-Ma lithosphere south of the fracture zone (Figure 7). In order to estimate the amount of yielding expected for each profile, we also computed the curvature of the plate at the first zero crossing seaward of the trench axis. At this location, the relationship between the bending moment supported by the plate and its curvature is independent of any applied in-plane stress [*McNutt and Menard*, 1982]. Average curvatures at the zero crossing K are $(2.4 \pm 0.6) \times 10^{-7}$ m^{-1} in the northern area and $(1.6 \pm 0.2) \times 10^{-7}$ m^{-1} in the south (Figure 7).

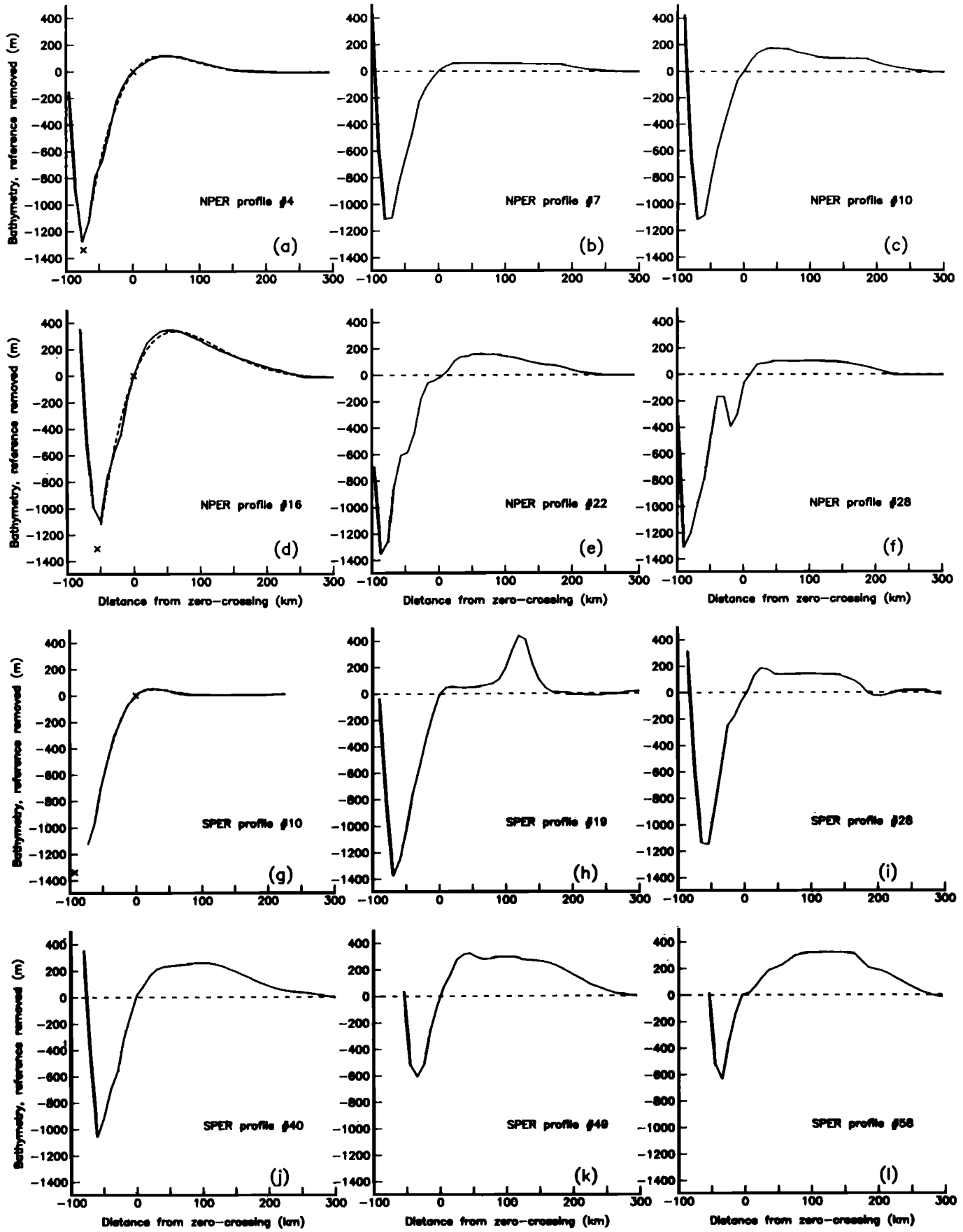

Fig. 4. A series of representative profiles across the Peru trench, extending 300 km to seaward and up to 70 km landward of the first zero crossing. NPER represents the northern region and SPER is the southern region. Those profiles which could be satisfactorily fit by the elastic model are shown with this model dashed in; those which could not are shown with a horizontal line at an estimated reference height.

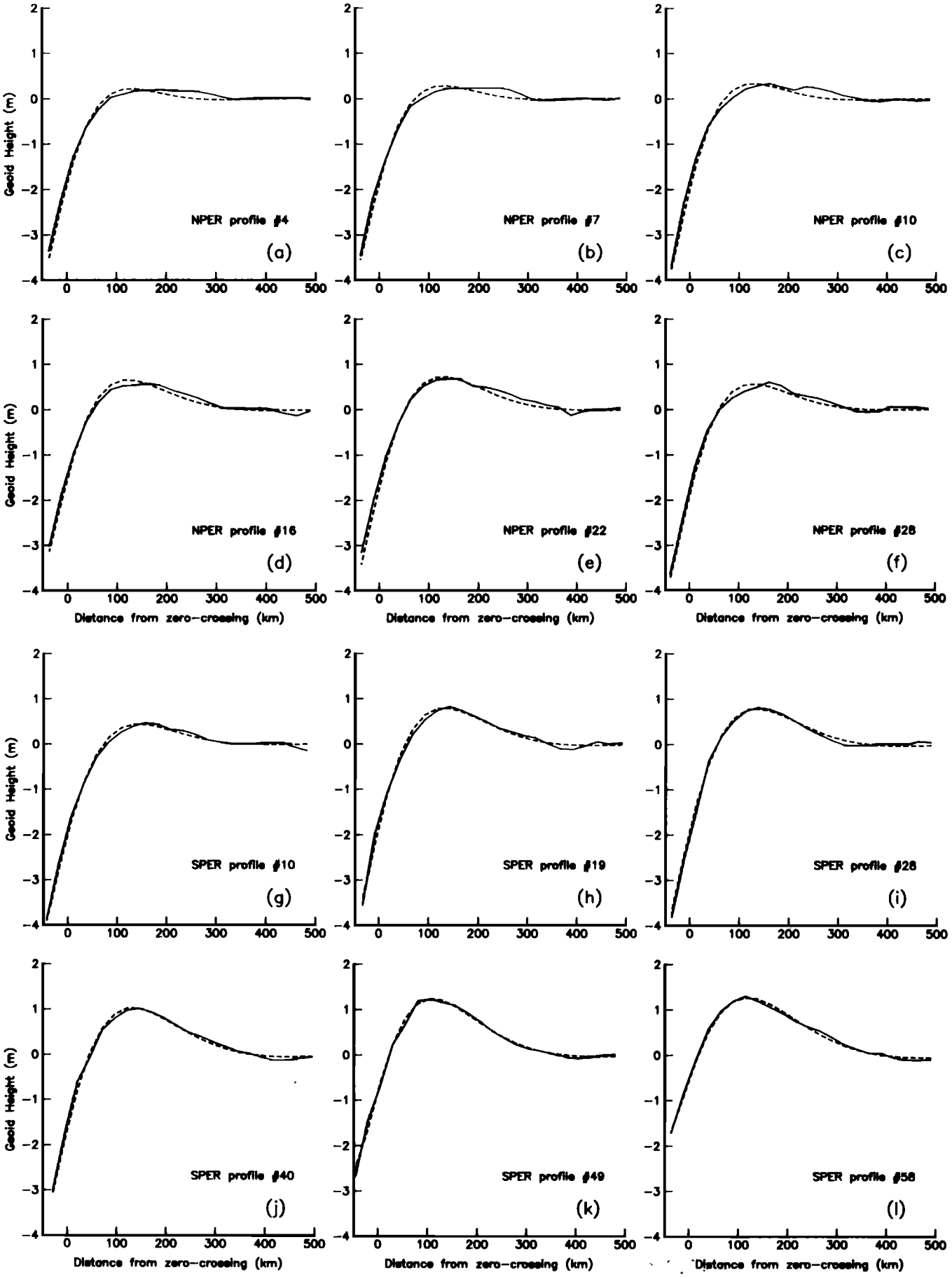

Fig. 5. The geoid along the same profiles for which bathymetry was shown in Figure 4. The solid line is the observed geoid, and the dashed line is the best fitting theoretical geoid which could be generated from an elastic curve.

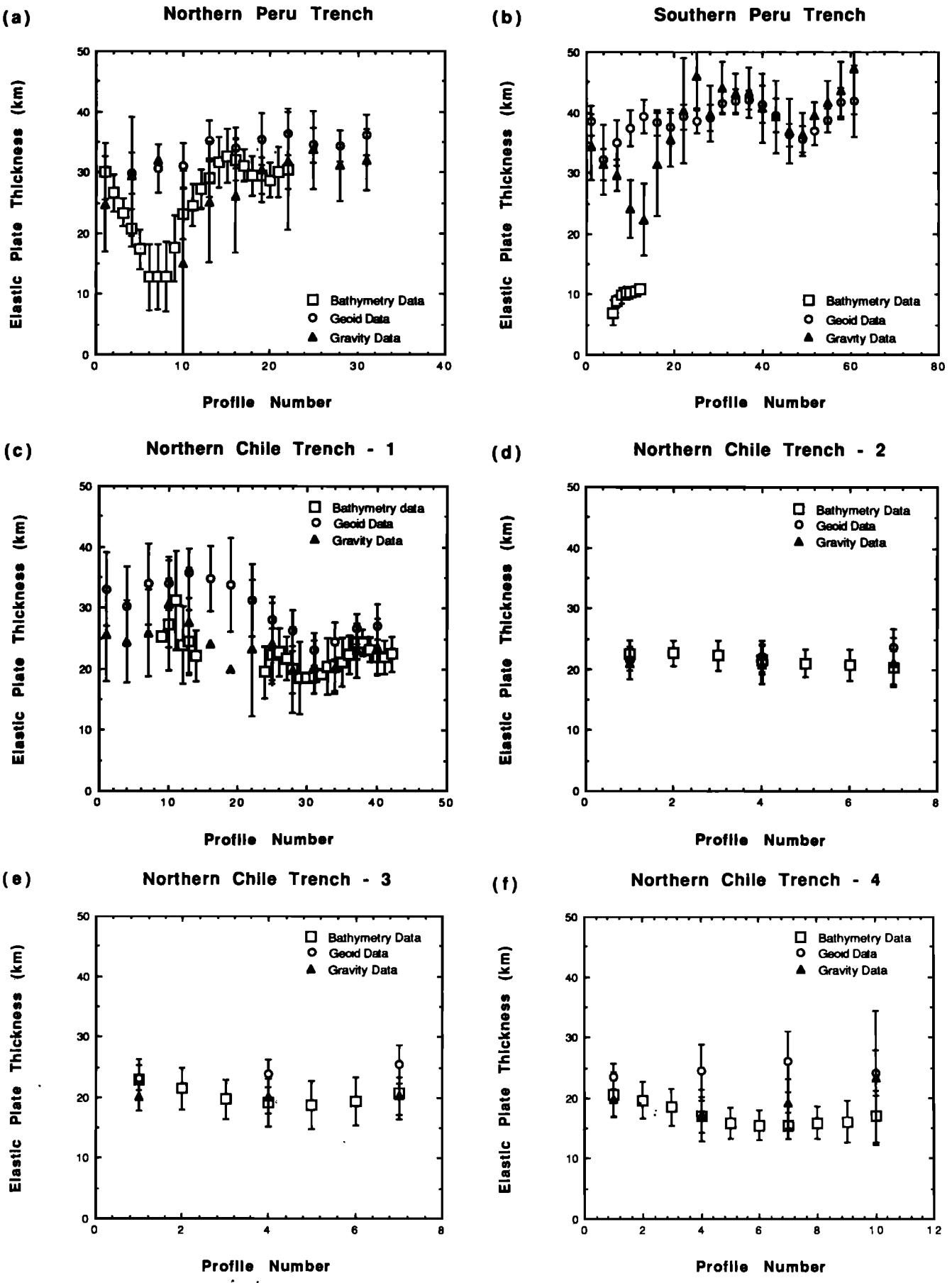

Fig. 6. Comparison of values of effective elastic thickness best fitting bathymetry, geoid, and gravity profiles within the two sections of the Peru Trench shown in Figure 3 and the five sections of the Chile Trench shown in Figure 8. Error bars give the uncertainty as determined from the half-width of the curve describing rms misfit as a function of T_e.

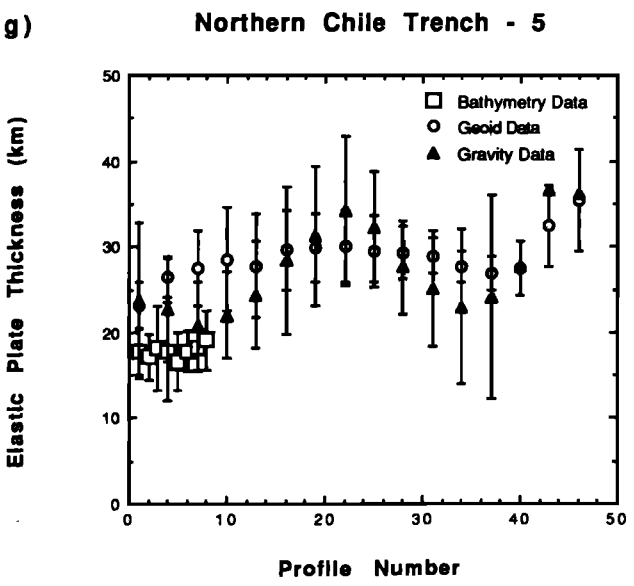

Fig. 6. (continued)

North Chile

The trench off northern Chile, from the Nazca ridge to 25°S, consists of two relatively straight segments separated by a short region with a radius of curvature of 310 km that we approximated as three short segments (Figure 8). The northernmost region 1 includes the northwest-southeast-trending 410-km-long portion of the trench lying immediately to the southeast of the Nazca ridge. The change in the dip of the slab occurs in the northwestern end of the region [*Barazangi and Isacks*, 1976, 1979]. In all of the profiles from the northern four of the five regions an outer bulge is apparent (Figures 9 and 10), and estimates of T_e computed from bathymetry, gravity, and geoid are fairly consistent (Figures 6*c* - 6*g*). Along the fifth segment of trench, except at its northern edge, the outer rise in the bathymetry is too rough to allow an estimate of T_e from bathymetry. The geoid and gravity signatures are less affected, and allow reasonable fits to plate flexure. Values for T_e derived from bathymetry, geoid, and gravity in Figures 6*c*–6*f* were used in computing the averages except along segment 5. We suspect that the digital bathymetric data base may not be as reliable as the satellite data in this southernmost region due to sparse ship tracks [*GEBCO*, 1980]. Average values for T_e and curvature of the plate in each segment are plotted in Figure 7.

Elastic Plates With Variable Rigidity

If inelastic processes caused by curvature-induced stresses produce failure in the plate, one would not expect the profiles to be completely described by an elastic profile with constant flexural rigidity. A look at those profiles best fit by elastic theory shows that this is the case. In both regions many of these profiles display a systematic deviation from the theoretical curves, with a more gradual slope to seaward of the bulge and a steeper slope landward of the peak than predicted by elastic theory. This often results in the observed position of the peak of the bulge being offset to landward of its predicted position.

The observed shape of these outer rises appears consistent with a model of a stiff plate which is weakened as it reaches the peak of the bulge. In order to model this effective thinning of an elastic plate brought on by failure, we used a finite difference algorithm that allows D to vary with position along the profile. The rigidity seaward of the peak of the outer rise was assumed constant and was derived from the flexural rigidity and curvature at the origin of the best fitting elastic curve by predicting the rigidity if no curvature and thus no thinning due to failure were present [*McNutt*, 1984], while the constant rigidity to landward and the exact position of the change in rigidity were chosen to best fit the observed profile. The results are shown for a profile off Peru in Figure 11*a* and for a profile off northern Chile in Figure 11*b*. In Peru the plate was best fit by an elastic thickness 5 km smaller landward of the bulge than to seaward, a decrease of 16%, whereas in northern Chile the plate was best fit by a model which thinned by more than a factor of 2. Allowing more than one rigidity change along a profile (Figure 11*c*) did not significantly improve the fit and sometimes led to physically unreasonable changes in rigidity, such as an increase in plate stiffness over the outer trench wall despite a corresponding increase in plate curvature.

The values of elastic thickness found earlier by considering each profile to be of constant rigidity can be considered weighted averages of the true elastic thickness along the length of the profile. These values, compared to the values found by modeling the profile with one change in flexural rigidity, are smaller than the elastic thickness on the seafloor, where no failure would be expected, but larger than that on the trench wall, near the zero-crossing. The values found when flexural rigidity is varied are similarly averages, but over smaller, arbitrarily chosen segments of the plate. At the Peru trench, profile 16 of the northern region is best fit by a constant 31.6-km-thick plate, or by a plate which changes in thickness from 32.8 and 27.6 km. Off northern Chile, profile 4 of region 2 is fit by a plate with a constant thickness of 21.5 km or by one which changes from 36.6 to 17.0 km. As the goal of this study is to understand the relationship between curvature-induced stresses and apparent elastic thickness, we wish to know if the curvature obtained by any elastic model is consistent with the plate thickness

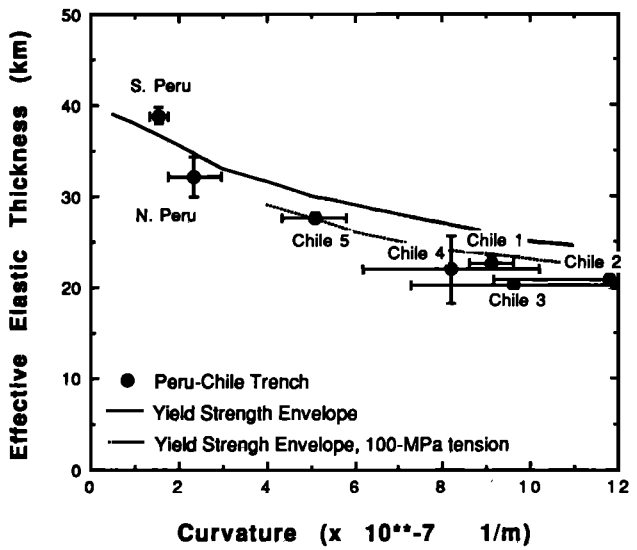

Fig. 7. Average values of elastic plate thickness within each of the seven sections of the Peru-Chile Trench plotted as a function of the curvature of the flexural profile at the first zero crossing seaward of the trench axis. The smooth line gives the predicted change in effective elastic thickness with increasing curvature for a more realistic rheology of the oceanic lithosphere that allows failure at high stress, as shown by the yield envelope in Figure 13 except with the elastic thickness of the plate extrapolated to zero curvature being 40 km. The dotted line gives the predicted reduction in elastic thickness if the lithosphere is subjected to 100 MPa of axial tension offshore northern Chile.

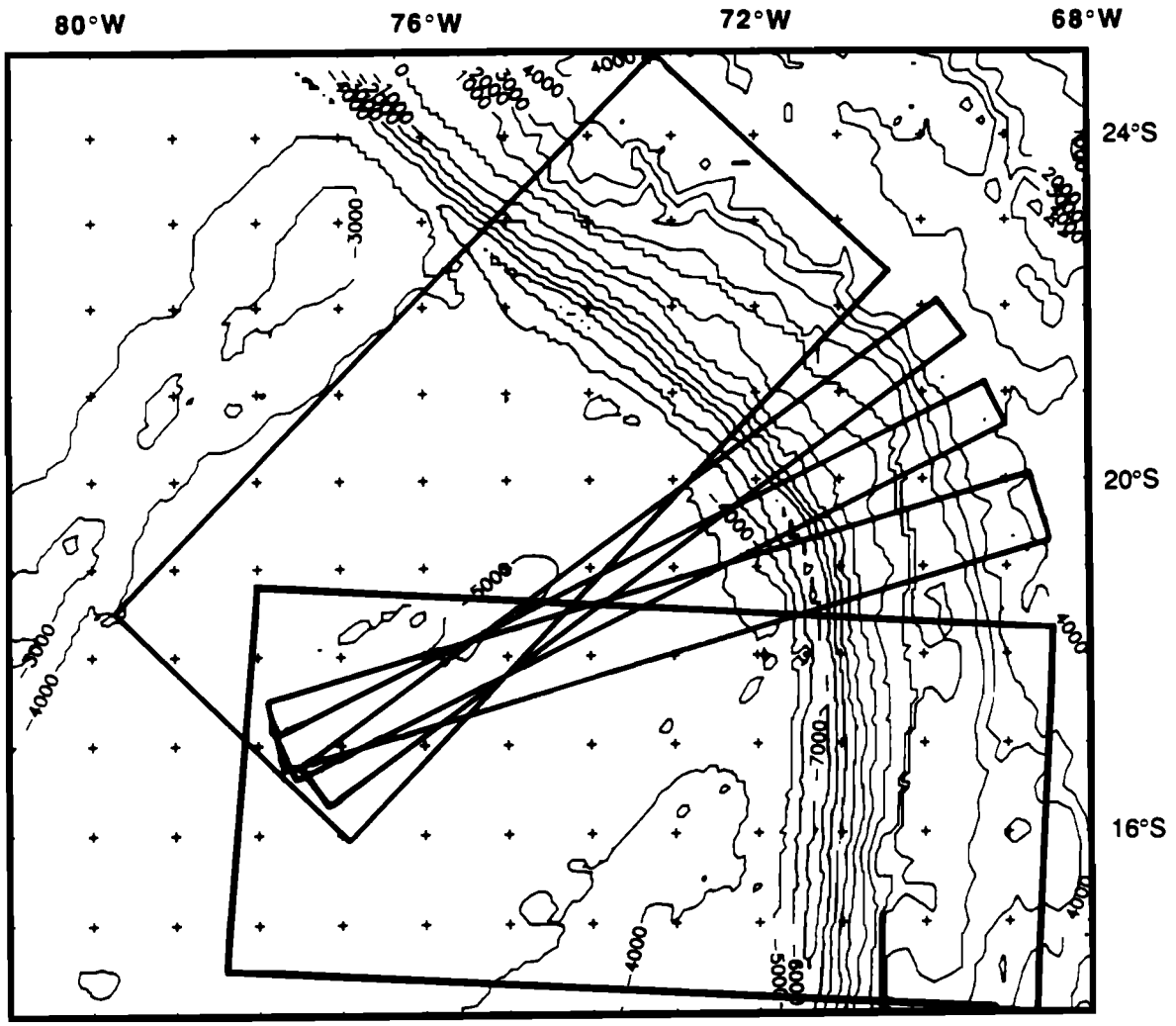

Fig. 8. Bathymetry of the region near the northern Chile Trench for which data were obtained, showing the location of the areas from which profiles were taken.

found according to that model at the point where curvature is measured. The curvatures of the profiles modeled here with variable rigidity were approximately 1.6 times their curvatures calculated assuming constant rigidity. This amount of change in curvature is consistent with the variation in elastic thickness at the zero-crossing as found by the two models [*McNutt*, 1984]. Therefore the values of elastic thickness found in this study should reflect the amount of thinning that the lithospheric plate is expected to undergo when it is bent to the calculated curvature.

Effect of In-Plane Stresses

In addition to a simple thinning of the plate with increasing curvature, horizontal compression or tension acting on the plate may influence the shape that it assumes. Lateral loads primarily affect the state of stress in the plate, though when large enough, it can affect the plate's shape. *McAdoo and Sandwell* [1985], in a study of the buckling of the lithosphere under the Indian Ocean, found that large compressive forces there have reduced the thickness of the elastic core of the plate to near one-tenth its full thickness. The effect of in-plane forces appears primarily in the measured thickness of the plate, not in the shape it assumes. Since the curvature of the bent plate is characterized by the remaining elastic core [*McAdoo and Sandwell*, 1985], we consider an elastic model a valid approximation of lithosphere entering a subduction zone, with horizontal loading serving to introduce another factor, in addition to plate curvature, which causes the effective elastic thickness of the plate to depart from its true mechanical thickness.

Three-Dimensional Effects

In the region of the Chile bight, where the strike of the trench changes over 45° within 175 km, the sharp turn in the trench may be affecting the shape and amplitude of the outer rise. The rise reaches peaks of over 1200 m, far larger than most outer rises, which are rarely larger than 600 m [*Caldwell et al.*, 1976; *Turcotte et al.*, 1978; *Jones et al.*, 1978; *Carey and Dubois*, 1981]. The bulge also has a gravity high of 80 mgal associated with it, which is larger than those observed over any other Pacific trench [*Schweller et al.*, 1981]. In the case of this much surface curvature in a trench, an approximation which treats it as a line load may not be valid. However, treating the trench as a cylindrical load of radius 350 km, using equations developed by *Brotchie* [1971], produced an elastic curve which best fit a profile off northern Chile that was nearly identical to the best fitting curve derived assuming a line load (Figure 12). The elastic parameters were slightly different in this case, with the elastic thickness which produced the best fitting cylindrical curve 1.5 km smaller, but this fell within the range of

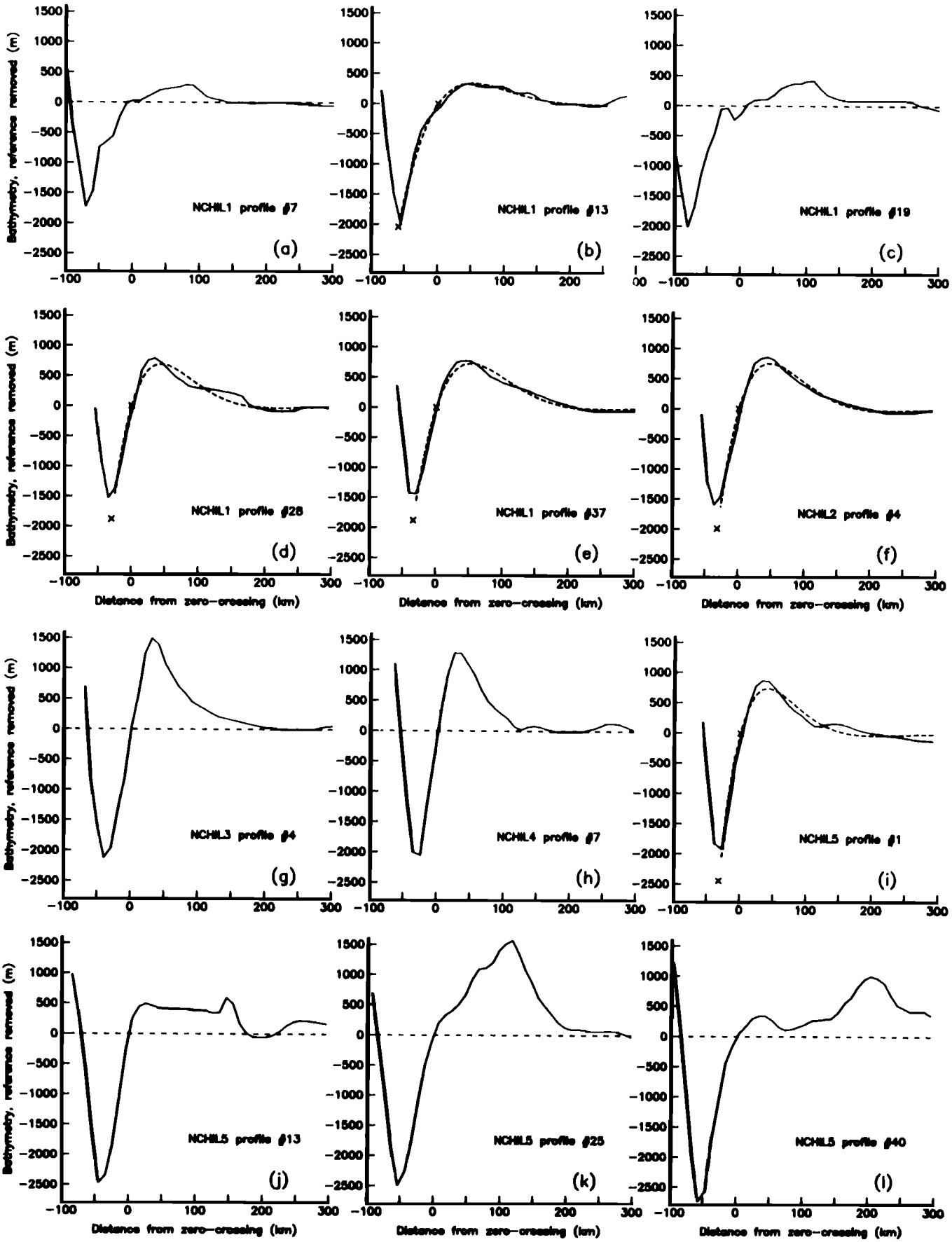

Fig. 9. A series of representative profiles across the northern part of the Chile trench, similar to those from the Peru Trench in Figure 4. NCHIL1 is region 1, NCHIL2 is region 2, and NCHIL3 is region 3. Those profiles which could be satisfactorily fit by the elastic model are shown with this model dashed in; those which could not are shown with a horizontal line at an estimated reference height.

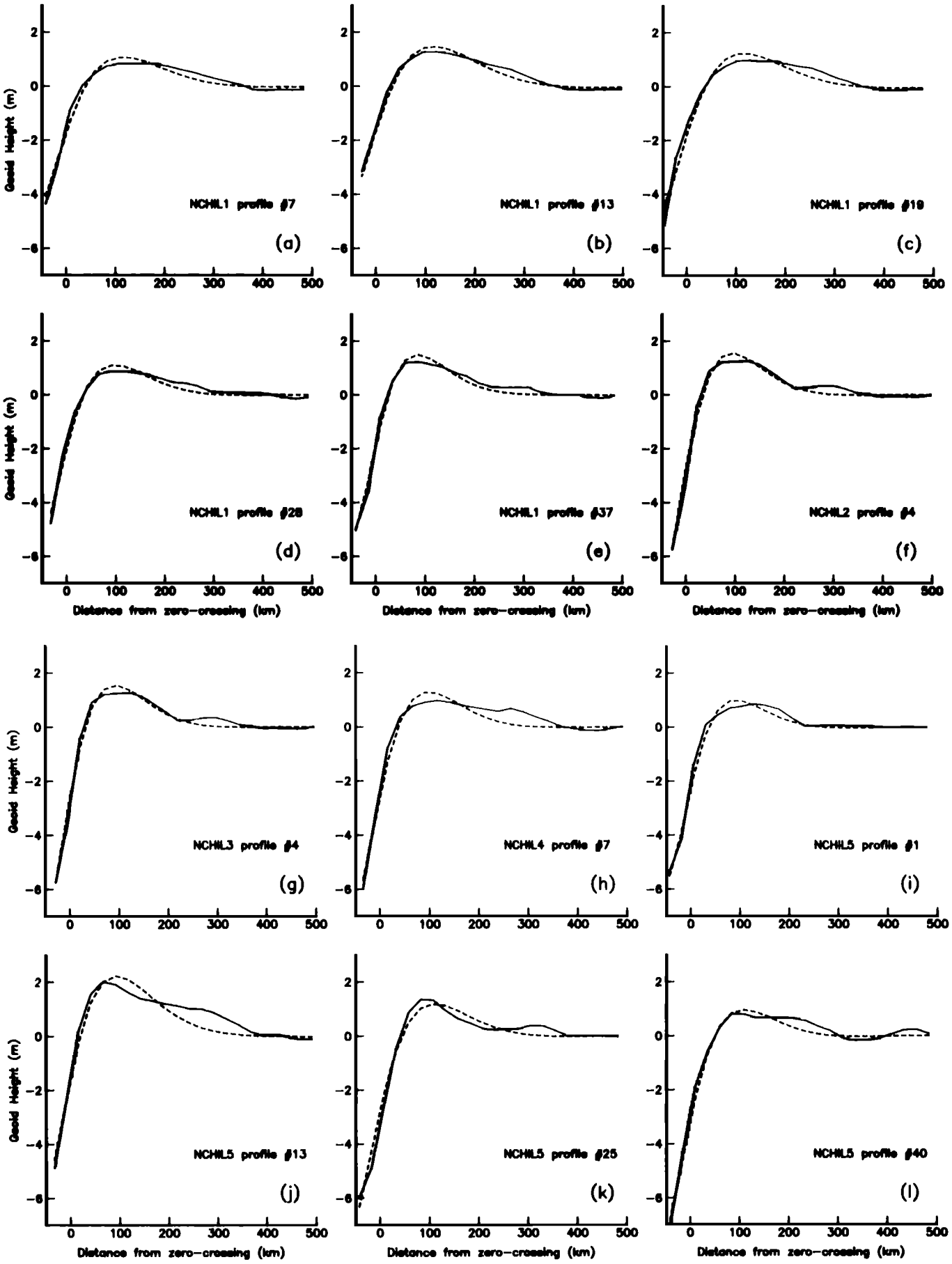

Fig. 10. The geoid along the same profiles for which bathymetry was shown in Figure 9. The solid line is the observed geoid, and the dashed line is the best fitting theoretical geoid generated from an elastic curve.

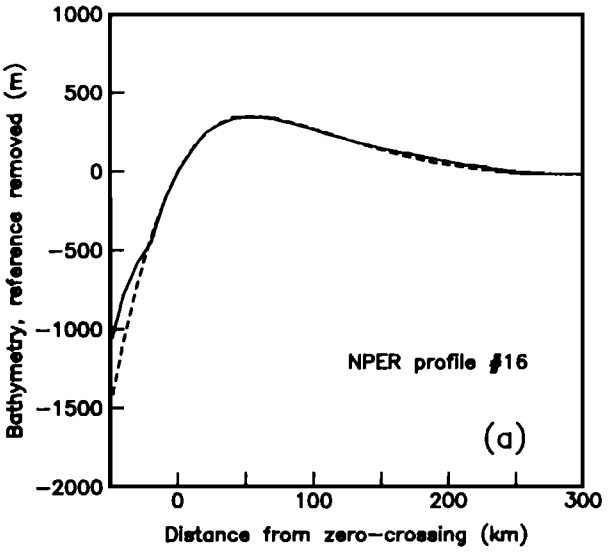

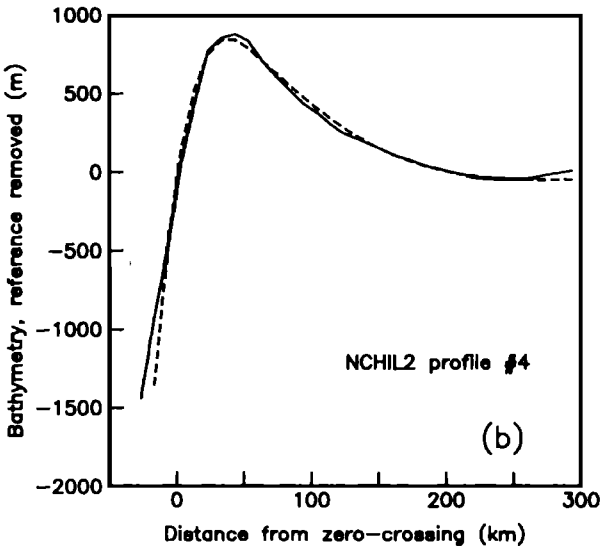

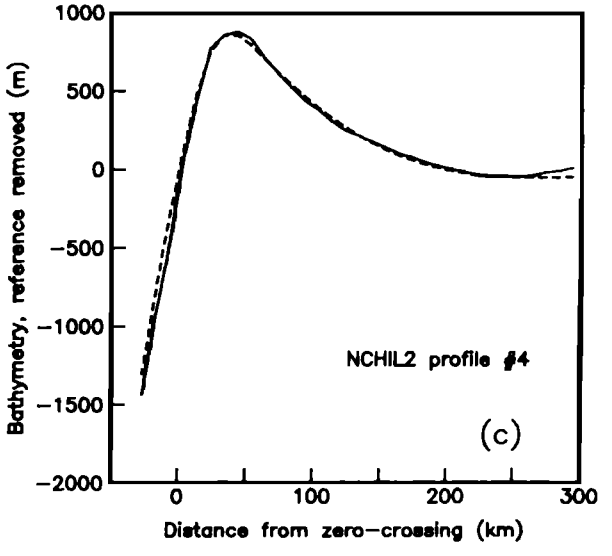

Fig. 11. Curves which result from modeling the bathymetry with an elastic plate of varying flexural rigidity. (*a*) The NPER profile 16 (solid line) shown with the curve which results when the flexural rigidity changes from 25 x 10^{22} Nm (T_e = 33 km) to 15 x 10^{22} Nm (T_e = 28 km) (dashed line). The change occurs 50 km seaward of the zero-crossing, with the larger rigidity occurring to seaward. The theoretical curve obtained assuming a constant rigidity is shown in Figure 4*d*. (*b*) The NCHIL2 profile 4 (solid line) shown with the curve which results when the flexural rigidity changes from 35 x 10^{22} Nm (T_e = 37 km) to 3.5 x 10^{22} Nm (T_e = 17 km) (dashed line). The change occurs 55 km seaward of the zero-crossing. The curve resulting from an elastic model with constant rigidity is shown in Figure 9*f*. (*c*) NCHIL2 profile 4 (solid line) shown with the curve which results when the flexural rigidity changes twice, from 35 x 10^{22} Nm (T_e = 37 km) greater than 70 km seaward of the zero-crossing, to 2.5 x 10^{22} Nm (T_e = 15 km) between 15 and 70 km seaward of the zero-crossing, to 15 x 10^{22} Nm (28 km) from x = 15 km to the trench (dashed line).

uncertainty in the elastic thickness determined earlier. It appears that if the sharp curvature of the trench has any effect on the shape of the plate, it cannot be modeled simply by changing the geometry of the load, and such complications can be safely ignored in favor of the model of a the two-dimensional line load.

Profiles Without Elastic Flexure

This discussion of means to better fit those profiles which could be explained by the elastic model neglects the many bathymetric profiles which could not be fit because of irregular seafloor in the region of the outer rise. *Erlandson et al.* [1981] have observed a region of rough basement along the entire area of the Peru-Chile Trench included in this study, extending 300 km seaward from the trench axis. The region shows evidence of faulting, upper crustal deformation, and volcanics, extending farther seaward than does the extensional faulting on the trench wall. They attribute these features to stresses encountered by the plate as it approaches the subduction zone. Regardless of the reason for this irregular bathymetry that masks the elastic behavior of the plate, the gravity and geoid data consistently indicate the presence of an outer rise along the Peru-Chile Trench.

DISCUSSION

Temperature at the Elastic-Ductile Transition

Along the Peru Trench, where the curvature of the plate is lower and therefore inelastic yielding should be less significant than further south, the average elastic thickness of the plate is 32 ± 2 km at 30 Ma and 39 ± 1 km at 42 Ma. If inelastic yielding can be completely ignored here and if the thermal structure of the Nazca plate in this region corresponds to the standard thermal plate model of *Parsons and Sclater* [1977], then these values of elastic plate thickness can be used to estimate the temperature Θ_e at the elastic-ductile transition. The *Parsons and Sclater* [1977] model predicts about 800 ± 50°C at the base of the elastic plate at these ages. Similar results were obtained by *McAdoo and Martin* [1984] and *McAdoo et al.* [1985], who modeled geoid data over nine trenches and found that Θ_e = 740°C. Studies of the focal depths of intraplate earthquakes [*Wiens and Stein*, 1983] also conclude that Θ_e = 800°C. If there is any inelastic yielding, then the actual depth to the elastic-ductile transition will be even greater, and the temperature even higher. This temperature agrees with that predicted for the elastic-ductile transition by simply extrapolating laboratory-derived flow laws to geologic strain rates [*Kirby*, 1980]. A temperature significantly lower than 700°C for the elastic-ductile transition would only be consistent with the data from the Peru Trench if the thermal structure of the Nazca plate is significantly colder than usual. The regional depth offshore Peru, however, is 4500 m,

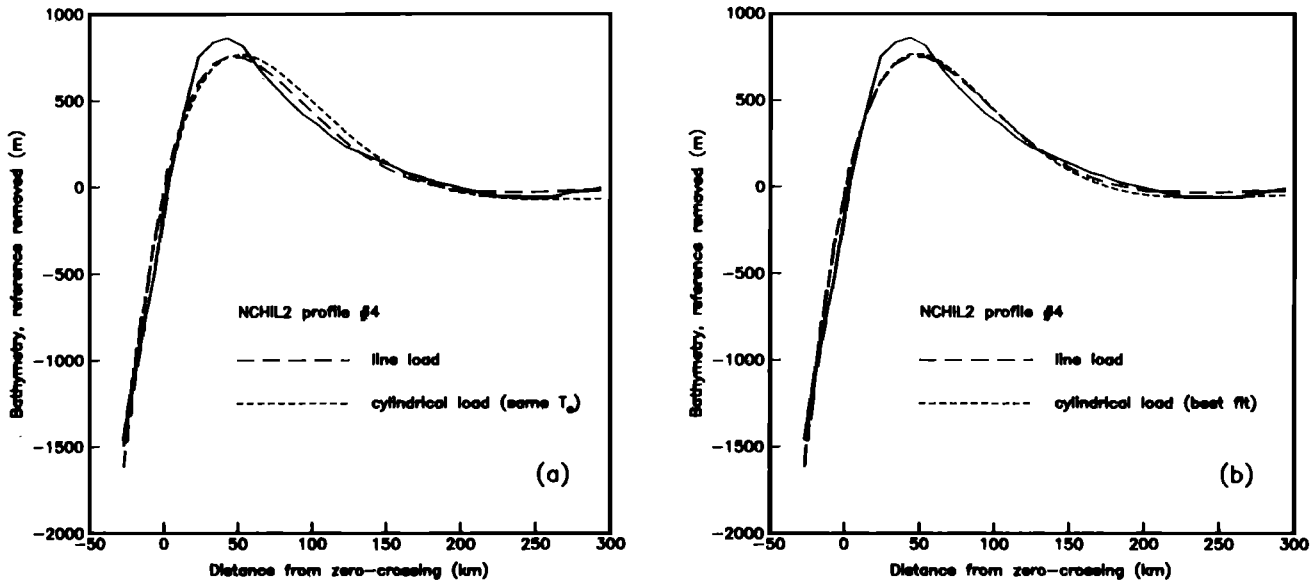

Fig. 12. Elastic curves resulting from a cylindrical load (short dashes) compared to that from a line load (long dashes) and the observed bathymetry (solid line) for NCHIL2 profile 4. The elastic curve produced by a line load uses the parameters which best fit the bathymetry (T_e = 21.4 km), and is that shown in Figure 9*f*. (*a*) The curve produced by a cylindrical load acting on a plate with the same elastic thickness as that acted on by the line load. (*b*) The curve produced by a cylindrical load which best fit the bathymetry, found using an elastic thickness of 19.8 km.

nearly the predicted value for normal 30-Ma lithosphere. Although there is no evidence at present that the thermal structure of the lithosphere is colder than average in this region, unusually hot thermal structure has been proposed as the explanation for the extremely small elastic plate thicknesses for French Polynesia just to the west of this study area [*McNutt and Fischer*, 1987]. We have proposed that a hot mantle upwelling is ultimately responsible for plate thinning [*McNutt and Judge*, 1990]. Perhaps the Nazca plate overlies the opposite limb of this convection cell, leading to colder lithosphere than usual. If further studies (using, for example, surface waves) determine that the thermal structure of the lithosphere is indeed normal in this region, then the fact that the effective elastic thickness of the lithosphere off Peru is so much greater than that found for lithosphere of similar age loaded by midplate volcanoes [*Watts et al.*, 1980] would imply that significant reheating of the lithosphere accompanies hot spot volcanism.

Inelastic Processes

The above discussion of T_e from the Peru Trench in terms of the depth to the isotherm at the elastic-ductile transition is predicated on the assumption that there is no inelastic yielding. However, the fact that the elastic plate thickness at North Chile is smaller (Figure 8) in spite of the greater lithospheric age suggests that inelastic yielding might be a factor, at least for North Chile if not for Peru. Apparently, at high plate curvature ($K > 5 \times 10^{-7}$ m^{-1}), the reduction in elastic plate thickness from such yielding can more than offset the expected increase in plate thickness over 15 m.y. of thermal cooling. Geologic evidence of faulting in and near the trench also supports the existence of yielding due to the curvature of the plate. Faulting on the outer trench wall is apparent in profiles taken along ship tracks across the Peru-Chile Trench [*Fisher and Raitt*, 1962; *Schweller et al.*, 1981]. These show numerous step faults and some graben structures. Step faults exist along the entire trench, with their average offset several hundred meters except in the North Chile region, where offsets of a kilometer exist [*Schweller et al.*, 1981]. Grabens appear primarily in the North Chile region. Evidence suggests that these features extend to depths of 4 to 7 km [*Schweller et al.*, 1981]. They reflect the failure that exists in the extensional, brittle upper zone of the plate. If this failure is the result of curvature-induced brittle failure, then it also suggests yielding at the base of the plate, although accomplished through different mechanisms (Figure 13).

In Figure 7 we compare the observed decrease in effective elastic thickness along the Peru-Chile Trench with that predicted from failure at high stresses of a lithosphere with finite yield strength as a function of depth given by a the yield envelope, such as that in Figure 13 [*McNutt*, 1984]. The impression from Figure 7 is that the lithosphere must be weaker than implied by the yield strength envelope in order to produce the observed amount of failure in the lithosphere when bent to high strains. Accounting for the expected increase of elastic plate thickness with increasing age would only increase the discrepancy in Figure 7 between the predicted and observed reduction in effective T_e. If, however, the stress field offshore northern Chile is characterized by tension normal to the trench axis at 16°S-27°S, but compression elsewhere, as has been proposed by *Wortel and Cloetingh* [1985] based on a finite element calculation incorporating plate-tectonic forces dependent on lithospheric age and kinematic parameters, additional weakening would be expected (Figure 7). Thus, although we are tempted to interpret our results as confirming the stress calculations of *Wortel and Cloetingh* [1985], we cannot rule out the possibility of thermal effects not predicted by lithospheric age. If, for example, the lithosphere is anomalously cold off Peru but normal off Chile, some of the reduction in T_e in Figure 7 may be controlled by temperature rather than state of stress.

Correlation Between Plate Dip and Elastic Thickness

Although a relationship between plate dip and the downward curvature of a plate is appealing, and the evidence from the Peru-Chile appears to support such a relationship, a further look at the region indicates that plate dip may not explain the variation in

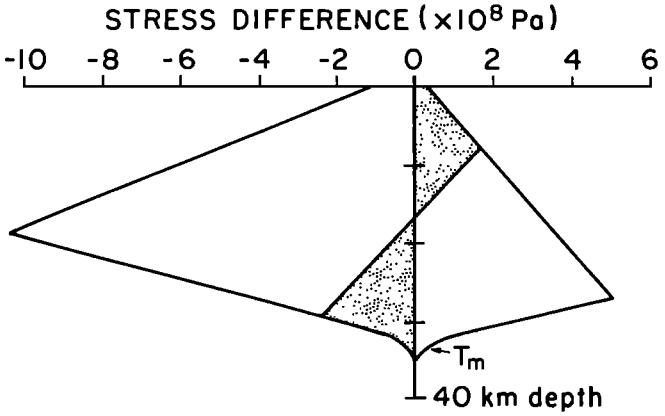

Fig. 13. An approximation of the yield envelope for a rheological model of the lithosphere which includes failure by frictional sliding at shallow depths and by ductile creep in the lower plate. T_m is the base of the mechanical lithosphere, assumed to correspond to the depth to an isotherm Θ_e. The inner line represents the stress difference due to flexure of such a plate that experiences yielding near the surface and base. The effective elastic thickness T_e of this plate computed by comparing its deformation to the predictions of the thin plate equation will always underestimate its true mechanical thickness T_m [from *McNutt*, 1984].

curvature, and therefore elastic thickness. The slope of the slab beneath Peru averages 15°, while beneath northern Chile it descends at approximately 33° [*Barazangi and Isacks*, 1976, 1979]. However, detailed analysis of the trends of the hypocentral surfaces indicates that in the upper 100 km the plate descends at the same slope in both regions, and then flattens under Peru while continuing to descend under northern Chile [*Bevis and Isacks*, 1984; *Chowdhury and Whiteman*, 1987]. Thus we find no support for a relationship between plate dip at depth and the elastic characteristics of that plate at the surface.

CONCLUSIONS

This investigation of the elastic thickness and curvature of the lithosphere entering the Peru-Chile Trench confirms the existence of a major change in many characteristics of the trench between the region lying off the coast of northern Peru from 6°S to 15°S and the region off the coast of northern Chile between 17°S and 20°S. The 30-m.y.-old plate off Peru appears to have an elastic thickness of 32 ± 2 km and a curvature of (2.4 ± 0.6) x 10^{-7} m^{-1}. It dips beneath the continent at 15°. The 45-m.y.-old plate off northern Chile has an elastic thickness of 23 ± 1 km, a curvature of (9.1 ± 0.5) x 10^{-7} m^{-1}, and dips at 33°. The older yet thinner plate of northern Chile indicates that the stresses induced by the curvature there are causing the plate to yield to a greater extent than occurs off Peru, where the smaller curvature induces correspondingly smaller stresses and less yielding. The presence of this failure in the plate is supported by the faulting observed on the outer trench wall, which is much more extensive in the sharply bent plate off Chile. However, it does not appear that the extreme downward curvature at the Chile Trench is related to the change in the dip of the plate at depth. Rather, it may be related to the intraplate stress field [*Wortel and Cloetingh*, 1985].

If the thermal structure of the lithosphere is normal for its age seaward of the Peru Trench, our results indicate that the isotherm defining the base of the mechanical lithosphere is 800° ± 50°C. This implies that the plate entering the North Chile Trench must be yielding to such an extent that the effective elastic thickness is approximately 50–65% of the plate's mechanical thickness, which is a larger amount of yielding than predicted by standard yield strength envelopes derived from laboratory experiments unless the intraplate stress field changes from offshore Peru to Chile [*Wortel and Cloetingh*, 1985]. In order to reconcile the relatively large elastic plate thickness for the Peru Trench with the results of lithospheric studies at midplate volcanoes, where stresses are lower and yielding should not occur, geotherms must be either significantly elevated beneath midplate swells [*McNutt*, 1984] or depressed offshore Peru.

Geoid heights and gravity anomalies show evidence of elastic flexure throughout the region studied, even in areas where the characteristic elastic profile is not evident in the bathymetry. In this respect it appears that geoid and gravity may be more reliable data sources for obtaining elastic plate thickness. However, where the bathymetry is well described by an elastic plate, values for elastic thickness obtained from the geoid are consistently larger than those obtained from bathymetry, an observation also made at numerous other subduction zones [*McAdoo and Martin*, 1984]. Such a systematic variation indicates that there may be characteristic subsurface density contrasts within a plate undergoing flexure which are reflected in the geoid but which are not apparent in the bathymetry, and that values of elastic thickness obtained from the two data sets should not be used interchangeably.

Acknowledgments. This paper benefitted from the constructive comments of four anonymous reviewers. This work was supported by National Science Foundation grant OCE-8710222.

REFERENCES

Barazangi, M., and B. L. Isacks, Spatial distribution of earthquakes and subduction of the Nazca plate beneath South America, *Geology*, *4*, 686–692, 1976.

Barazangi, M., and B. L. Isacks, Subduction of the Nazca plate beneath Peru: Evidence from spatial distribution of earthquakes, *Geophys. J. R. Astron. Soc.*, *57*, 537–555, 1979.

Bevis, M., and B. L. Isacks, Hypocentral trend surface analysis: Probing the geometry of Benioff zones, *J. Geophys. Res.*, *89*, 6153–6170, 1984.

Bodine, J. H., and A. B. Watts, On lithospheric flexure seaward of the Bonin and Mariana trenches, *Earth Planet. Sci. Lett.*, *43*, 132–148, 1979.

Brotchie, J. F., Flexure of a liquid-filled spherical shell in a radial gravity field, *Mod. Geol.*, *3*, 15–23, 1971.

Caldwell, J. G., W. F. Haxby, D. E. Karig, and D. L. Turcotte, On the applicability of a universal elastic trench profile, *Earth Planet. Sci. Lett.*, *31*, 239–246, 1976.

Carey, E., and J. Dubois, Behavior of the oceanic lithosphere at subduction zones: Plastic yield strength from a finite-element method, *Tectonophysics*, *74*, 99–110, 1981.

Chowdhury, D. K., and S. K. Whiteman, Structure of the Benioff zone under southern Peru to central Chile, *Tectonophysics*, *134*, 215–226, 1987.

Dang, S., Seismic refraction velocity structure, Sheet 9, in *Peru-Chile Trench Off Peru*, Ocean Margin Drilling Program, Regional Atlas Series, Atlas *9*, edited by D.M. Hussong, S.P. Dang, L.D. Kulm, R.W. Couch, and T.W.C. Hilde, Marine Science International, Woods Hole, Mass., 1984.

Erlandson, D. L., D. M. Hussong, and J. F. Campbell, Sediment and associated structure of the northern Nazca plate, Nazca Plate: Crustal Formation and Andean Convergence, *Mem. Geol. Soc. Am.*, *154*, 295–314, 1981.

Fisher, R. L., and R. W. Raitt, Topography and structure of the Peru-Chile trench, *Deep Sea Res.*, *9*, 423–443, 1962.

GEBCO, Bathymetric Chart of the Oceans, 1:10,000,000, 5th ed., Canadian Hydrographic Office, Ottawa, Canada, 1980.

Goetze, C., and B. Evans, Stress and temperature in the bending lithosphere as constrained by experimental rock mechanics, *Geophys. J. R. Astron. Soc.*, *59*, 463–478, 1979.

Handschumacher, D. W., Post-Eocene plate tectonics of the eastern

Pacific, in *The Geophysics of the Pacific Ocean Basin and its Margin, Geophys. Monogr. Ser.*, vol. 19, edited by G.H. Sutton, M.H. Manghnani, and R. Moberly, pp 177–202, AGU, Washington, D.C., 1976.

Hanks, T. C., The Kuril Trench-Hokkaido Rise system: Large shallow earthquakes and simple models of deformation, *Geophys. J. R. Astron. Soc., 23*, 173–189, 1971.

Haxby, W.F., *Gravity Field of the World's Oceans*, National Geophysical Data Center, NOAA, Boulder, Colo., 1987.

Heirtzler, J. R., and M. Edwards, Relief of the surface of the Earth, *Rep. MGG-2*, Nat. Geophys. Data Cent., Boulder, Colo., 1985.

Herron, E. M., Sea-floor spreading and the Cenozoic history of the East Central Pacific, *Geol. Soc. Am. Bull., 83*, 1671–1692, 1972.

Hilde, T. W. C., and W. E. K. Warsi, Magnetic anomaly profiles, Sheet 4, in *Peru-Chile Trench Off Peru*, Ocean Margin Drilling Program, Regional Atlas Series, Atlas *9*, edited by D.M. Hussong, S.P. Dang, L.D. Kulm, R.W. Couch, and T.W.C. Hilde, Marine Science International, Woods Hole, Mass., 1984.

Hussong, D. M., P. B. Edwards, S. H. Johnson, J. F. Campbell, and G. H. Sutton, Crustal structure of the Peru-Chile Trench: 8°–12° S latitude, in *The Geophysics of the Pacific Ocean Basin and its Margin, Geophys. Monogr. Ser.*, vol. 19, edited by G.H. Sutton, M.H. Manghnani, and R. Moberly, pp 71-85, AGU, Washington, D.C., 1976.

Jones, G. M., T. W. C. Hilde, G. F. Sharman, and D. C. Agnew, Fault patterns in outer trench walls and their tectonic significance, *J. Phys. Earth, 26*, Suppl., S 85–S 101, 1978.

Kirby, S. H., Tectonic stresses in the lithosphere: Constraints provided by the experimental deformation of rocks, *J. Geophys. Res., 85*, 6353–6363, 1980.

Marsh, J. G., A. C. Brenner, B. D. Beckley, and T. V. Martin, Global mean sea surface based upon the Seasat altimeter data, *J. Geophys. Res., 91*, 3501–3506, 1986.

Marsh, J. G., F. J. Lerch, B. H. Putney, D. C. Christodoulidis, D. E. Smith, T. L. Felsentreger, B. V. Sanchez, S. M. Klosko, E. C. Pavlis, T. V. Martin, J. W. Robbins, R. G. Williamson, O. L. Colombo, D. D. Rowlands, W. F. Eddy, N. L. Chandler, K. E. Rachlin, G. B. Patel, S. Bhati, and D. S. Chinn, A new gravitational model for the Earth from satellite tracking data: GEM-T1, *J. Geophys. Res., 93*, 6169–6215, 1988.

McAdoo, D. C., and C. F. Martin, Seasat observations of lithospheric flexure seaward of trenches, *J. Geophys. Res., 89*, 3201–3210, 1984.

McAdoo, D. C., and D. T. Sandwell, Folding of oceanic lithosphere, *J. Geophys. Res., 90*, 8563–8569, 1985.

McAdoo, D. C., J. G. Caldwell, and D. L. Turcotte, On the elastic-perfectly plastic bending of the lithosphere under generalized loading with application to the Kuril Trench, *Geophys. J. R. Astron. Soc., 54*, 11–26, 1978.

McAdoo, D. C., C. F. Martin, and S. Poulose, Seasat observations of flexure: Evidence for a strong lithosphere, *Tectonophysics, 116*, 209–222, 1985.

McNutt, M. K., Lithospheric flexure and thermal anomalies, *J. Geophys. Res., 89*, 11,180–11,194, 1984.

McNutt, M.K., and K.M. Fisher, The South Pacific superswell, in *Seamounts, Islands, and Atolls, Geophys. Monogr. 43*, edited by B. Keating, P. Fryer, R. Batiza, and G.W. Boehlert, AGU, Washington, D.C., 1987.

McNutt, M.K., and A.V. Judge, The superswell and mantle dynamics beneath the South Pacific, *Science, 248*, 969–975, 1990.

McNutt, M. K., and H. W. Menard, Constraints on yield strength in the oceanic lithosphere derived from observations of flexure, *Geophys. J. R. Astron. Soc., 71*, 363–394, 1982.

Parker, R. L., The rapid calculation of potential anomalies, *Geophys. J. R. Astron. Soc., 31*, 447–455, 1972.

Parsons, B. E., and J. Sclater, An analysis of the variation of ocean floor bathymetry and heat flow with age, *J. Geophys. Res., 82*, 803–827, 1977.

Scheidegger, K. F., and J. B. Corliss, Petrogenesis and secondary alteration of upper layer 2 basalts of the Nazca plate, Nazca Plate: Crustal Formation and Andean Convergence, *Mem. Geol. Soc. Am., 154*, 77–107, 1981.

Schweller, W. J., L. D. Kulm, and R. A. Prince, Tectonics, structure, and sedimentary framework of the Peru-Chile Trench, Nazca Plate: Crustal Formation and Andean Convergence, *Mem. Geol. Soc. Am., 154*, 323–349, 1981.

Turcotte, D. L, and G. Schubert, *Geodynamics: Applications of Continuum Physics to Geological Problems*, John Wiley, New York, 1982.

Turcotte, D. L, D. C. McAdoo, and J. G. Caldwell, An elastic-perfectly plastic analysis of the bending of the lithosphere at a trench, *Tectonophysics, 47*, 193–205, 1978.

Walcott, R. I., Flexure of the lithosphere at Hawaii, *Tectonophysics, 9*, 435–446, 1970.

Watts, A. B., and J. R. Cochran, Gravity anomalies and flexure of the lithosphere along the Hawaiian–Emperor Seamount Chain, *Geophys. J. R. Astron. Soc., 38*, 119–141, 1974.

Watts, A. B., J. H. Bodine, and N. M. Ribe, Observations of flexure and the geological evolution of the Pacific Ocean basin, *Nature, 283*, 532–537, 1980.

Wiens, D. A., and S. Stein, Age dependence of oceanic intraplate seismicity and implications for lithospheric evolution, *J. Geophys. Res., 88*, 6455–6468, 1983.

Wortel, M.J.R., and S.A.P.L. Cloetingh, Accretion and lateral variations in tectonic structure along the Peru-Chile trench, *Tectonophysics, 112*, 443–462, 1985.

A.V. Judge, Geophysical Research, ELF Aquitaine, CSTCS avenue Larribou, 64018 Pau Cedex, FRANCE.

M.K. McNutt, 54-826 MIT, Cambridge, MA 02139

(Received July 19, 1988;
revised July 30, 1990;
accepted August 7, 1990.)